DE LA RECHERCHE À L'INDUSTRIE

# Three-dimensional hydrodynamic interaction of two-coaxial cylinders

***Maria Adela PUSCAS*** [1]
*Romain Lagrange* [2]

[1] *CEA/DES/ISAS/DM2S/STMF/LMSF*
[2] *CEA/DES/ISAS/DM2S/SEMT/DYN*

Séminaire d'Informatique Scientifique et de Mathématiques Appliquées

19/05/2022

# Contents

# FSI problem of a body vibrating in a fluid

- Mechanics of plants and trees
- Understanding of animal swimming
- Energy harvesting from a flexible structure
- *Steam generator in a nuclear Pressurized Water Reactor (PWR)*
- **Jules Horowitz Reactor (JHR)**

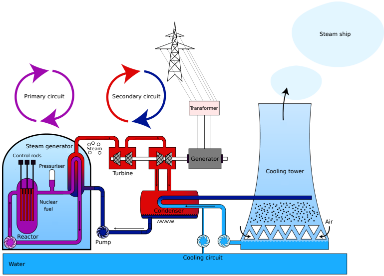


(a) PWR design

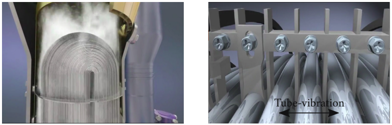


(b) Steam generator

# FSI problem of a body vibrating in a fluid

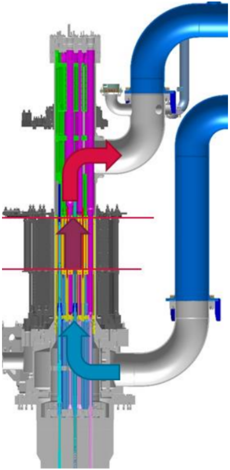

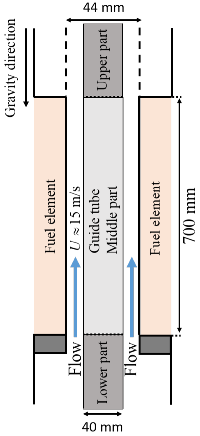


FIGURE – Left : sketch of the **Jules Horowitz Reactor (JHR)**. Right : axial cross section of the JHR assembly cell.

## Fluid is initially at rest
## New theoretical formulation and numerical validation

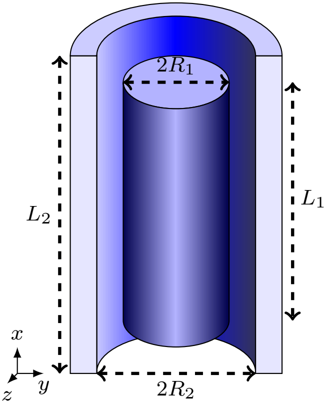


FIGURE – Schematic diagram of the system

- Two coaxial oscillating cylinders $\mathcal{C}_j$ with radii $R_j$ and length $L_i$
- Immersed in a fluid of kinematic viscosity $\nu$
- Imposed displacement $\Re\left\{e^{i\Omega T}\mathbf{Q}_i(X)\right\}$

$$\mathbf{Q}_i(X) = Q\,\frac{W_i(X)}{N_i}\mathbf{e}_y,$$

$\Omega$ the angular frequency,
$Q$ the amplitude of the displacement,
$W_i(X)$ the $i$-th bending mode of vibration of an Euler-Bernoulli beam

$$W_i(X) = \chi^{(1)}\cosh(\Lambda_i X) + \chi^{(2)}\cos(\Lambda_i X) + \chi_i^{(3)}\sinh(\Lambda_i X) + \chi_i^{(4)}\sin(\Lambda_i X),$$

$$N_i = \sup\left(|W_i(X)|, X \in [0, L]\right).$$

# Governing equations

The Navier-Stokes equations and the boundary conditions for the incompressible fluid flow $\Re\left\{\mathrm{e}^{\mathrm{i}\Omega T}(\mathbf{V}_i, P_i)\right\}$ generated by the displacement $\mathbf{Q}_i$ write

$$\begin{aligned}
\nabla \cdot \mathbf{V}_i &= 0, \\
\mathrm{i}\Omega \mathbf{V}_i + \left(\Re\left\{\mathrm{e}^{\mathrm{i}\Omega T}\mathbf{V}_i\right\} \cdot \nabla\right)\mathbf{V}_i + \frac{1}{\rho}\nabla P_i - \nu \Delta \mathbf{V}_i &= \mathbf{0}, \\
\mathbf{V}_i - \mathrm{i}\Omega \mathbf{Q}_i &= \mathbf{0} \quad \text{on } \partial C_1, \\
\mathbf{V}_i &= \mathbf{0} \quad \text{on } \partial C_2.
\end{aligned}$$

The linear fluid force $\Re\left\{\mathrm{e}^{\mathrm{i}\Omega T}\mathbf{F}_i\,(X)\right\}$ acting on $\mathcal{C}_1$ writes

$$\mathbf{F}_i = -\int_{\partial^\Gamma C_1} P_i \mathbf{n}_1 d\Gamma + \rho\nu \int_{\partial^\Gamma C_1} \left[\nabla \mathbf{V}_i + (\nabla \mathbf{V}_i)^{\mathrm{T}}\right] \cdot \mathbf{n}_1 d\Gamma,$$

The modal added-mass coefficient $M_{ij}$ is defined as the projection of the fluid force component $\mathbf{F}_i \cdot \mathbf{e_y}$ generated by the $i$-th mode $W_i/N_i$ onto the $j$-th mode $W_j/N_j$

$$M_{ij} = \frac{1}{N_j}\Re\left\{\frac{\langle \mathbf{F}_i \cdot \mathbf{e}_y, W_j\rangle}{Q\Omega^2}\right\}, \quad \text{with } \langle F, G\rangle = \int_0^L F(X)G(X)dX.$$

# Governing equations

Dimensionless Navier-Stokes equations

$$
\begin{aligned}
\nabla^* \cdot \mathbf{v}_i &= 0, \\
\mathrm{i}\mathbf{v}_i + \frac{KC}{\varepsilon - 1}\left(\mathbf{v}_i \cdot \nabla^*\right)\mathbf{v}_i + \frac{1}{\varepsilon - 1}\nabla^* p_i - \frac{1}{Sk}\left(\frac{1}{\varepsilon - 1}\right)^2 \Delta^* \mathbf{v}_i &= \mathbf{0}, \\
\mathbf{v}_i - \mathrm{i}\mathbf{q}_i &= \mathbf{0} \quad \text{on } \partial C_1, \\
\mathbf{v}_i &= \mathbf{0} \quad \text{on } \partial C_2,
\end{aligned}
$$

- $x = X/L_1$ and $t = T\Omega$
- $\mathbf{V}_i = Q\Omega\, \mathbf{v}_i$, $P_i = \rho Q R_1 \Omega^2\, p_i$, $\mathbf{F}_i = \rho Q \left(R_1 \Omega\right)^2\, \mathbf{f}_i$
- $\mathbf{q}_i = \mathbf{Q}_i/Q$ and $w_i\left(x\right) = W_i\left(L_1 x\right)$
- $\nabla^* = \left(R_2 - R_1\right)\nabla$ and $\Delta^* = \left(R_2 - R_1\right)^2 \Delta$
- Aspect ratio $l = \dfrac{L_1}{R_1}$ and radius ratio $\varepsilon = \dfrac{R_2}{R_1}$
- Keulegan-Carpenter number $KC = \dfrac{Q}{R_1}$ and Stokes number $Sk = \dfrac{{R_1}^2\Omega}{\nu}$

# The fluid coupled modes with different wave-numbers

- The inner cylinder is imposed a vibration mode corresponding to a **clamped-free** boundary condition :

$$w_i(x) = \cosh(\lambda_i x) - \cos(\lambda_i x) - \sigma_i (\sinh(\lambda_i x) - \sin(\lambda_i x))$$

- **Slender-body theory** [M. P. Païdoussis, Dynamics of cylindrical structures subjected to axial flow, 1973]

$$m_{ij}^{(\mathrm{ref},\infty)}(\varepsilon) = \frac{\varepsilon^2+1}{\varepsilon^2-1}\frac{\langle w_i, w_i\rangle}{N_i^2}\delta_{ij}$$

- 3D numerical simulations with **TrioCFD** : $R_1 = 0.02$ m, $R_2 = 0.022$ m, $L_1 = 0.7$ m, $L_2 = 0.8$m, $Q = 5 \times 10^{-5}$ m, and $\Omega/(2\pi) = 90$ Hz

| **Clamped – Free** | Slender – body theory, $m_{ij}^{(\mathrm{ref},\infty)}$ | Numerics TrioCFD | Relative deviation (%) |
|---|---|---|---|
| | $\begin{pmatrix} 2.631 & 0 & 0 \\ 0 & 2.631 & 0 \\ 0 & 0 & 2.631 \end{pmatrix}$ | $\begin{pmatrix} 2.475 & 0.2391 & -0.2067 \\ 0.2405 & 2.463 & 0.2232 \\ -0.2081 & 0.2241 & 2.410 \end{pmatrix}$ | 10 .0 |

FIGURE – Dimensionless added mass matrix for the clamped-free case. The radius ratio is $\varepsilon = 1.1$ and the aspect ratio is $l = 35$

- The numerical **added mass matrix** is **non-diagonal**, with off-diagonal terms of the order of $10\%$ of the diagonal terms

# New theoretical formulation

# New theoretical formulation

- Neglect the viscous effects : $Sk \to \infty$
- Small oscillations (neglect the nonlinear convective term) : $KC \to 0$
- Dimensionless Navier-Stokes equations simplifies to

$$\begin{aligned}
\nabla^* \cdot \mathbf{v}_i &= 0, \\
\mathrm{i}\mathbf{v}_i + \frac{1}{\varepsilon - 1} \nabla^* p_i &= \mathbf{0}, \\
(\mathbf{v}_i - \mathrm{i}\mathbf{q}_i) \cdot \mathbf{n}_1 &= 0 \quad \text{on } \partial C_1, \\
\mathbf{v}_i \cdot \mathbf{n}_2 &= 0 \quad \text{on } \partial C_2.
\end{aligned}$$

- The pressure field is a harmonic function

$$\Delta^* p_i = \frac{\partial^2 p_i}{\partial r^2} + \frac{1}{r}\frac{\partial p_i}{\partial r} + \frac{1}{r^2}\frac{\partial^2 p_i}{\partial \theta^2} + \frac{1}{l^2}\frac{\partial^2 p_i}{\partial x^2} = 0,$$

with $(r, \theta, x) = (R/R_1, \theta, X/L)$ the dimensionless cylindrical coordinates.

# New theoretical formulation

- Introducing $\tilde{r} = r - 1$, $\tilde{p_i}\left(\tilde{r}, \theta, x\right) = p_i\left(r - 1, \theta, x\right)$, and $1/r \approx 1$ (**narrow annulus**)

$$\frac{\partial \tilde{p_i}}{\partial \tilde{r}} + \frac{\partial^2 \tilde{p_i}}{\partial \theta^2} + \frac{1}{l^2}\frac{\partial^2 \tilde{p_i}}{\partial x^2} = -\frac{\partial^2 \tilde{p_i}}{\partial \tilde{r}^2}.$$

- Averaging in the radial direction of the annulus

$$\left\langle \frac{\partial \tilde{p_i}}{\partial \tilde{r}} \right\rangle_{\tilde{r}} + \frac{\partial^2 \left\langle \tilde{p_i} \right\rangle_{\tilde{r}}}{\partial \theta^2} + \frac{1}{l^2}\frac{\partial^2 \left\langle \tilde{p_i} \right\rangle_{\tilde{r}}}{\partial x^2} = -\frac{1}{\varepsilon - 1}\left[\frac{\partial \tilde{p_i}}{\partial \tilde{r}}\right]_{\tilde{r}=0}^{\tilde{r}=\varepsilon-1}, \text{ with } \left\langle \tilde{p_i} \right\rangle_{\tilde{r}} = \frac{1}{\epsilon - 1}\int_0^{\varepsilon-1} \tilde{p_i}\, d\tilde{r}.$$

- Using the boundary conditions

$$\left.\frac{\partial \tilde{p_i}}{\partial \tilde{r}}\right|_{\tilde{r}=0} = -\mathbf{i}\mathbf{v}_i \cdot \mathbf{e}_r \approx -\mathbf{i}\mathbf{v}_i \cdot \mathbf{n}_1 = \frac{w_i}{N_i}\cos\left(\theta\right), \qquad \left.\frac{\partial \tilde{p_i}}{\partial \tilde{r}}\right|_{\tilde{r}=\varepsilon-1} = 0.$$

# New theoretical formulation

- Seeking a solution as $\langle \tilde{p_i} \rangle_{\tilde{r}} = \overline{p_i}\,(x)\,/N_i \cos(\theta)$

$$\frac{d^2\overline{p_i}}{dx^2} - l^2\overline{p_i} = \frac{1}{\varepsilon - 1} l^2 w_i.$$

- Modeled the cylinder as an Euler-Bernoulli beam :

$$w_i\,(x) = \chi^{(1)} \cosh(\lambda_i x) + \chi^{(2)} \cos(\lambda_i x) + \chi_i^{(3)} \sinh(\lambda_i x) + \chi_i^{(4)} \sin(\lambda_i x)\,.$$

- The dimensionless pressure in the narrow channel writes

$$p_i\,(x,\theta) \underset{\varepsilon\to 1}{\sim} = -\sum_{k=1}^{2} \left[ g_i^{(k)}\,(x,l,\varepsilon) + a_i^{(k)}\,(l,\varepsilon)\,\mathrm{e}^{lx} + b_i^{(k)}\,(l,\varepsilon)\,\mathrm{e}^{-lx} \right] cos(\theta).$$

- The dimensionless fluid force writes

$$\mathbf{f}_i = \underset{\varepsilon\to 1}{\sim} (\varepsilon - 1)\,\frac{1}{\pi} \int_0^1 \int_0^{2\pi} -p_i\,(x,\theta)\mathbf{e}_r d\theta dx.$$

⇒ **New theoretical formulation** for the dimensionless **modal added mass** coefficient

$$m_{ij}\left(l,\varepsilon,w_i,w_j\right)=\frac{1}{\varepsilon-1}\left[m_{ij}^{(S)}\left(l,w_i,w_j\right)+m_{ij}^{(A)}\left(l,w_i,w_j\right)\right]$$

- Depends on the radius ratio $\varepsilon$, the aspect ratio $l$, and the vibration mode $w_j$
- Full analytical expressions for $m_{ij}^{(S)}$ and $m_{ij}^{(A)}$
- Applies for all classical boundary conditions

**R. Lagrange** and **M. A Puscas**
New theoretical and numerical results on the modal added-mass matrix of a finite length flexible cylinder immersed in a narrow annular fluid, considering various boundary conditions.
Journal of Fluids and Structures, submitted, 2022.

**R. Lagrange** and **M. A Puscas**
Hydrodynamic interaction between two flexible finite length coaxial cylinders : new theoretical formulation and numerical validation.
Journal of Applied Mechanics, submitted, 2022.

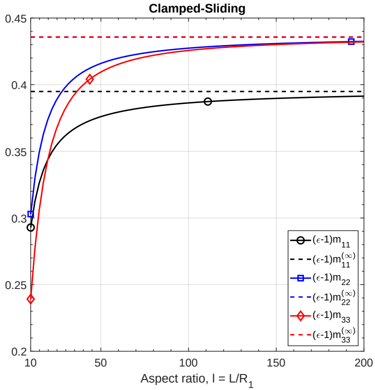


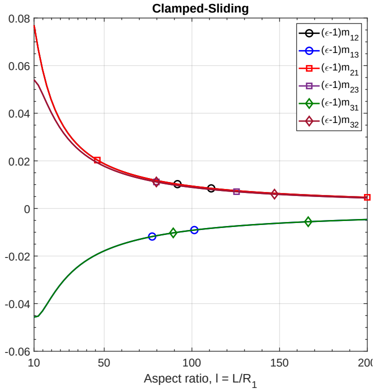


FIGURE – **Clamped-Sliding** case. Evolution of the added mass coefficient $(\varepsilon - 1)m_{ij}$ as a function of the aspect ratio $l$. Left : diagonal terms. The horizontal dashed lines correspond to the limit $l \to \infty$. Right : off-diagonal terms

# Fluid solver

# Incompressible turbulent fluid solver : TrioCFD software

- A Computational Fluid Dynamics code developed at CEA for incompressible or quasi-compressible turblent flows and energy transfert
- Two spatial discretizations : “Finite Difference-Volume" (FDV) for square/hexahedral meshes and “Finite Element-Volume" (FEV) for triangular/tetrahedral meshes
  Note : the PolyMAC discretization on the polygonal mesh will be soon available
- Time discretization schemes : explicit (Forward Euler) and implicit (Backward Euler) whitin a multi-step (projection-correction) technique
- RANS and LES turbulence models
- Eulerian formulation
- **Open source** (http ://triocfd.cea.fr/) and massively parallel (SPMD + MPI).

# TrioCFD with Arbitrary Lagrangian-Eulerian framework

- Imposed displacement on the inner cylinder in the form $\mathbf{Q}(X)\sin(\Omega T)$
- The numerical simulation does not neglect the convective and viscous terms of the Navier-Stokes equations
- The FSI problem involving moving boundaries is solved using an Arbitrary Lagrange-Eulerian method (ALE)
- A fluid particle is identified by its position relative to a frame moving with a nonuniform velocity $\mathbf{V}_{ALE}$

$$
\begin{aligned}
\nabla \cdot \mathbf{V} &= 0, \\
\frac{\partial J \mathbf{V}}{\partial T} - J\left(\nu \Delta \mathbf{V} - (\mathbf{V} \cdot \nabla)\,\mathbf{V} + (\mathbf{V_{ALE}} \cdot \nabla)\,\mathbf{V} - \frac{1}{\rho}\nabla P\right) &= \mathbf{0}, \\
\mathbf{V} - \Omega \mathbf{Q}(X)\cos(\Omega T) &= \mathbf{0} \quad \text{on } \partial C_1, \\
\mathbf{V} &= \mathbf{0} \quad \text{on } \partial C_2,
\end{aligned}
$$

where $J$ is the Jacobian of the transformation between the ALE and the Lagrange descriptions.

# TrioCFD with Arbitrary Lagrangian-Eulerian (ALE) framework

- Many possibilities to calculate $\mathbf{v}_{ALE}$. For moderate deformations, one can pose a Laplace problem that is known as harmonic mesh motion [Donea, Giuliani, Halleux, CMAME, 1982] :

$$
\begin{aligned}
\Delta \mathbf{V}_{ALE} &= \mathbf{0}, \\
\mathbf{V}_{ALE} - \Omega \mathbf{Q}(X)\cos(\Omega T) &= \mathbf{0} \quad \text{on } \partial C_1, \\
\mathbf{V}_{ALE} &= \mathbf{0} \quad \text{on } \partial C_2,
\end{aligned}
$$

- Discretisation : hybrid Finite Element-Volume method for tetrahedral grids and the first-order backward Euler scheme

$$
\begin{aligned}
[D]\mathbf{V}_h{}^{n+1} &= \mathbf{0}, \\
[M]\frac{\left(J^{n+1}\mathbf{V}_h{}^{n+1} - J^n \mathbf{V}_h{}^n\right)}{\Delta t} - J^{n+1}\Big([A]\mathbf{V}_h{}^{n+1} - [L(\mathbf{V}_h{}^n)]\mathbf{V}_h{}^{n+1} + & \\
[L(\mathbf{V}_h{}^n)]\mathbf{V}_{h,ALE}{}^{n+1} - [G]P_h{}^{n+1}\Big) &= \mathbf{0},
\end{aligned}
$$

$[D]$, $[M]$, $[A]$, $[L(\mathbf{V})]$, and $[G]$ the discrete divergence, mass, diffusion, nonlinear, and gradient matrix operators.

- FEV method : a modification of the Crouzeix-Raviart element (P1NC/P0 EF).
- The discrete pressure is defined on the primary grid while the discrete velocity is defined on a face-based staggered dual grid.
- Local equations are integrated over control volumes : the primal mesh cells for mass and the dual mesh cells for impulsion.
- Fluxes and differential operators are computed by means of a Finite Elements (FE) formulation.
- Three FEV schemes resulting from the choice of the pressure DoF : P1NC/P0, P1NC/P0+P1 and P1NC/P0+P1+Pa.

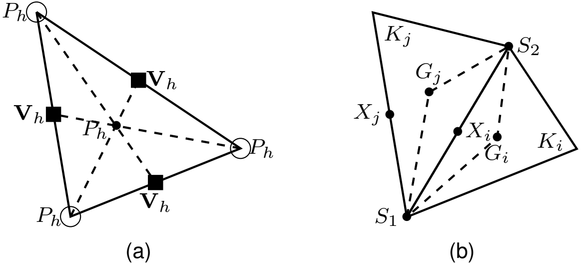


FIGURE – (a)Degrees of freedom of a 2D element (black squares for velocity $\mathbf{V}_h$, black dots and circles for pressure $P_h$). (b) Dual control volume between two adjacent triangular cells $K_i$ and $K_j$ of respective barycenters $G_i$ and $G_j$.

# Theory vs. Numerics

# Comparison to numerical simulations : effect of the radius ratio

| **Clamped – Free** | Present theory | Numerics TrioCFD | Relative deviation (%) |
|---|---|---|---|
| $\varepsilon = 1.0375$ | $\begin{pmatrix} 5.939 & 0.6682 & -0.5841 \\ 0.6682 & 5.937 & 0.6098 \\ -0.5841 & 0.6098 & 5.838 \end{pmatrix}$ | $\begin{pmatrix} 6.370 & 0.6695 & -0.5732 \\ 0.6576 & 6.324 & 0.6063 \\ -0.5724 & 0.6034 & 6.185 \end{pmatrix}$ | 6.11<br>3.20 |
| $\varepsilon = 1.1$ | $\begin{pmatrix} 2.227 & 0.2506 & -0.2190 \\ 0.2506 & 2.227 & 0.2287 \\ -0.2190 & 0.2287 & 2.189 \end{pmatrix}$ | $\begin{pmatrix} 2.475 & 0.2391 & -0.2067 \\ 0.2405 & 2.463 & 0.2232 \\ -0.2081 & 0.2241 & 2.410 \end{pmatrix}$ | 10.0<br>5.95 |
| $\varepsilon = 1.2$ | $\begin{pmatrix} 1.114 & 0.1253 & -0.1095 \\ 0.1253 & 1.113 & 0.1143 \\ -0.1095 & 0.1143 & 1.095 \end{pmatrix}$ | $\begin{pmatrix} 1.278 & 0.1164 & -0.09944 \\ 0.1172 & 1.269 & 0.1098 \\ -0.1007 & 0.1112 & 1.239 \end{pmatrix}$ | 12.8<br>8.73 |

FIGURE – Dimensionless added mass matrix for the **clamped-free** case and three values of the **radius ratio** $\varepsilon = \{1.0375, 1.1, 1.2\}$. The aspect ratio is $l = 35$.

$R_1 = 0.02$ m, $\Omega/(2\pi) = 90$ Hz, and $Q = K\,(R_2 - R_1)$, with $K = 2.5$ %

# Comparison to numerical simulations : effect of the aspect ratio

| Clamped – Free | Present theory | Numerics TrioCFD | Relative deviation (%) |
|---|---|---|---|
| $l = 35$ | $\begin{pmatrix} 2.227 & 0.2506 & -0.2190 \\ 0.2506 & 2.227 & 0.2287 \\ -0.2190 & 0.2287 & 2.189 \end{pmatrix}$ | $\begin{pmatrix} 2.475 & 0.2391 & -0.2067 \\ 0.2405 & 2.463 & 0.2232 \\ -0.2081 & 0.2241 & 2.410 \end{pmatrix}$ | 10.0<br>5.95 |
| $l = 70$ | $\begin{pmatrix} 2.360 & 0.1341 & -0.1261 \\ 0.1341 & 2.360 & 0.1285 \\ -0.1261 & 0.1285 & 2.350 \end{pmatrix}$ | $\begin{pmatrix} 2.603 & 0.1267 & -0.1191 \\ 0.1278 & 2.598 & 0.1238 \\ -0.1199 & 0.1243 & 2.584 \end{pmatrix}$ | 9.33<br>5.88 |
| $l = 140$ | $\begin{pmatrix} 2.429 & 0.06920 & -0.06720 \\ 0.06920 & 2.429 & 0.06780 \\ -0.06720 & 0.06780 & 2.427 \end{pmatrix}$ | $\begin{pmatrix} 2.682 & 0.06520 & -0.06380 \\ 0.06590 & 2.681 & 0.06500 \\ -0.06390 & 0.06520 & 2.677 \end{pmatrix}$ | 10.2<br>5.70 |

FIGURE – Dimensionless added mass matrix for the **clamped-free** case and three values of the **aspect ratio** $l = \{35, 70, 140\}$. The radius ratio is $\varepsilon = 1.1$.

$R_1 = 0.02$ m, $\Omega/(2\pi) = 90$ Hz, and $Q = K\,(R_2 - R_1)$, with $K = 2.5$ %

# Comparison to numerical simulations : aspect ratio

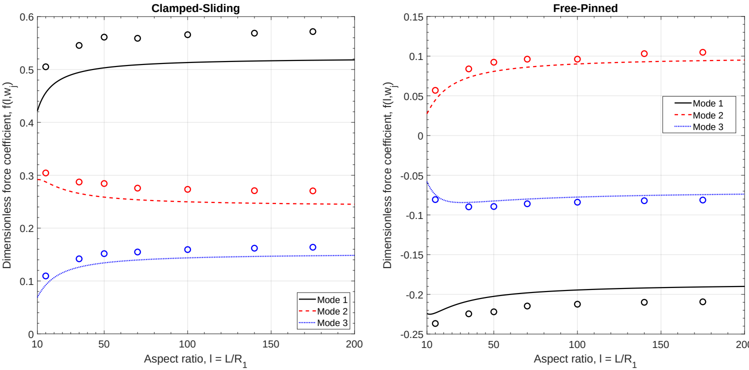


FIGURE – Evolution of the dimensionless fluid force $(\varepsilon - 1)(\mathbf{f}_j \cdot \mathbf{e}_y) = f(l, w_j)$, as a function of the **aspect ratio**, $l = L/R_1 \in \{15, 35, 50, 70, 100, 140, 175\}$, for the first three modes of the **clamped-sliding** and **free-pinned** boundary conditions. The radius ratio is $\varepsilon = 1.1$. Lines correspond to the theoretical prediction and open circles correspond to the numerical simulations.

Axial flow.
CFD solver coupled
with a beam structure

# Bending vibration of a beam

- Structural dynamics :

$$M\ddot{u}(x,t) + C\dot{u}(x,t) + Ku(x,t) = F_f(x,t) \qquad (6)$$

- $F_f(x,t)$ the fluid force
- The matrices $M$ and $K$ are computed based on a spatial finite element discretization (the beam element, polynomial approximation of degree 3)
- $C$ is computing by the following equation (Rayleigh damping) :

$$C = \alpha M + \omega K, \quad \text{where } \alpha \text{ and } \omega \text{ are two parameters of the method}$$

- Model reduction method for the dynamic response analysis of a beam structure

$$u(x,t) = \sum_{j=0}^{m} q_j(t) w_j(x) \qquad (7)$$

- The modal deformations $w_j$ are computed by solving an eigenvalue problem :

$$(K - \lambda^2 M)w(x) = 0$$

By introducing the decomposition (7) into the equilibrium equation (6), by multiplying by $w_j$ and integrating along the beam, we get **m independent scalar equations** :

$$m_j \ddot{q}_j(t) + c_j \dot{q}_j(t) + k_j q_j(t) = f_j(t),\ j = 0, \dots, m.$$

with :

- $f_j(t) = \int_0^1 F_f(x,t) w_j(x) dx$ (projection of the fluid force on the mode $j$)
- $m_j = w_j(x)^T M w_j(x)$ (projection of the mass matrix on the mode $j$)
- $m_{ij} = w_i(x)^T M w_j(x) = 0$ (orthogonality of modes). Idem for $c_{ij}$ and $k_{ij}$

Vectorial form :

$$M^* \ddot{q}(t) + C^* \dot{q}(t) + K^* q(t) = f(t),$$

with $M^* = diag(m_0, \dots, m_m)$, $C^* = diag(c_0, \dots, c_m)$, etc.

# Temporal discretization

- Temporal discretization is based on the Newmark family integration schemes :

$$\begin{cases} \left(M^* + \gamma\Delta t C^* + \beta\Delta t^2 K^*\right)\ddot{q}^{n+1} = f^{n+1}(\dot{q}^{n+1}) - C^*\left(\dot{q}^n + (1-\gamma)\Delta t\ddot{q}^n\right) \\ \qquad - K^*\left(q^n + \Delta t\dot{q}^n + \Delta t^2\left(\frac{1}{2} - \beta\right)\ddot{q}^n\right) \\ \dot{q}^{n+1} = \dot{q}^n + (1-\gamma)\Delta t\ddot{q}^n + \gamma\Delta t\ddot{q}^{n+1} \\ q^{n+1} = q^n + \Delta t\dot{q}^n + \Delta t^2\left(\frac{1}{2} - \beta\right)\ddot{q}^n + \Delta t^2\beta\ddot{q}^{n+1} \end{cases}$$

Centered differences

- $\gamma = 1/2$, $\beta = 0$
- **Explicit** scheme
- The scheme is stable if $\Delta t \leq \Delta t_{crit}$ with $\Delta t_{crit} \leq 2\frac{l_c}{c}$

Average acceleration

- $\gamma = 1/2$, $\beta = 1/4$
- **Implicit** scheme
- The scheme is unconditionally stable

# TrioCFD coupling with the reduced beam model

- Recombine on physical basis $u^{n+1}(x,t) = \sum_{j=0}^{m} q_j^{n+1} w_j(x)$
- **Interpolations** on the 3d surface of the fluid-structure interface
- **Explicit** (or loosely coupling) **time coupling** scheme between TrioCFD and the beam model : **conventional serial staggered** (CSS) scheme.

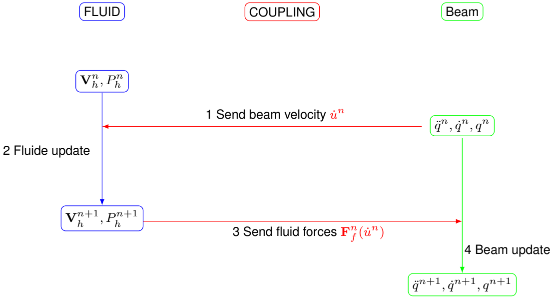


FIGURE – Structure of the **explicit CSS** coupling scheme

# Laminar flow. Pinned - pinned case

- $R_1 = 0.02$ m, $R_1 = 0.022$ m, $L_1 = 0.7$ m, $L_2 = 0.8$ m, $\Omega/(2\pi) = 90$ Hz
- Explicit CSS time coupling scheme between TrioCFD and the beam model. Initial condition for the beam : release of $0.1$ mm and boundary condition of type pinned-pinned.
- **Slender-body theory** [M. P. Païdoussis and M.Ostoja-Starzewski, Slender flexible cylinder in an incompressible axial flow theory, 1981]
- Modal added mass coefficient $m_{11}$ :

| Reynolds | Theory | CSS | $\tau(\%)$ |
|---|---|---|---|
| 0 | 5.388 | 5.480 | 1.7 |
| 100 | 5.388 | 5.480 | 1.7 |
| 200 | 5.388 | 5.481 | 1.7 |
| 500 | 5.388 | 5.486 | 1.8 |
| 1000 | 5.388 | 5.480 | 1.7 |
| 2000 | 5.388 | 5.471 | 1.5 |

FIGURE – Dimensionless added mass coefficient $C_{m,11}$ for the pinned - pinned case. The radius ratio is $\varepsilon = 1.1$, the aspect ratio is $l = 35$, and the frequency $\Omega/(2\pi) = 90$ Hz.

- Reynolds, $Re = \dfrac{2(R_2 - R1)\overline{V}_{ann}}{\nu}$

# Turbulent flow : URANS simulations. Pinned - pinned case

- URANS $k - \epsilon$ model
- $R_1 = 0.02$ m, $R_1 = 0.022$ m, $L_1 = 0.7$ m, $L_2 = 0.8$ m, $\Omega/(2\pi) = 90$ Hz
- Explicit CSS time coupling scheme between TrioCFD and the beam model. Initial condition for the beam : release of $0.1$ mm and boundary condition of type pinned-pinned.
- Modal added mass coefficient $m_{11}$ :

| Reynolds | Theory | CSS | $\tau(\%)$ |
|---|---|---|---|
| 0 | 5.388 | 5.356 | 0.59 |
| $4 \cdot 10^4$ | 5.417 | 5.402 | 0.27 |
| $5 \cdot 10^4$ | 5.431 | 5.422 | 0.16 |
| $6 \cdot 10^4$ | 5.455 | 5.479 | 0.43 |

FIGURE – Dimensionless added mass coefficient $C_{m,11}$ for the pinned - pinned case. The radius ratio is $\varepsilon = 1.1$, the aspect ratio is $l = 35$, and the frequency $\Omega/(2\pi) = 90$ Hz.

# Conclusions and perspectives

Conclusions :

- New theoretical formulation to estimate the fluid force and the added mass matrix
  - Good agreement between the numerics and the new theoretical formulation
  - Different classical types of the boundary conditions ($3$ first modes)
  - Effect of the radius ratio : $\varepsilon \in \{1.0375, 1.1, 1.2\}$
  - Effect of the aspect ratio : $l \in \{15, 35, 50, 70, 100, 140, 175\}$
  - Vibration of the inner *and* external cylinders
- Explicit time coupling between TrioCFD (ALE) and a beam structure model
  - Good agreement for the mass coefficients
  - Laminar flow : $Re \in \{0, 100, 200, 500, 1000, 2000\}$
  - Turbulent flow : $Re \in \{4 \cdot 10^4, 5 \cdot 10^4, 6 \cdot 10^4\}$

Perspectives :

- Refine the present theory further to consider the **viscous effects** (working in progress) : derive analytical expressions for the added-mass and **added-damping**
- Derive analytical expressions for the fluid forces due to an **axial flow**
- Carry out an **analysis of stability** to establish the Argand's diagrams of all the boundary conditions
- Focus on the effect of the off-diagonal terms generated by the finite length of the vibrating cylinder on the threshold of instability

Thank you for your attention